Earth's Ionosphere and its Impact on Global Navigation Satellite Systems

S. Skone and M. Najmafshar
University of Calgary

1. ABSTRACT

Global Navigation Satellite System (GNSS) technologies are susceptible to space weather effects, and are rapidly evolving with multiple constellations available from Europe, the Unites States, Russia and China. Positioning, navigation and timing (PNT) accuracies are approaching the threshold of sub-centimeter globally, with a multitude of new services from precision timing to unmanned systems and drones. Integrity must now extend from traditional safety-critical navigation systems (e.g. aviation and marine) to ubiquitous autonomous platform applications and beyond. There is a growing focus to ensure that current and future GNSS services are robust and reliable during severe space weather and the associated ionospheric disturbances.

There are multiple phenomena that produce space weather impacts on GNSS: the introduction of large gradients in the ionospheric total electron content (TEC); the rapid variation of a signal's amplitude and/or phase (scintillation); and/or the sudden increase in background L-band noise. Often such effects are reduced through dual-frequency ionosphere-free combinations, models, and/or differential techniques. Structured features in TEC and small-scale plasma irregularities are difficult to reduce or mitigate, however, and the larger PNT errors can challenge integrity of navigation solutions. For example, we have observed the storm-enhanced density phenomenon, and associated tongue of ionization at Arctic latitudes, generating ten-fold increases in GNSS positioning errors exceeding system thresholds. Scintillations in the Canadian Arctic have resulted in loss of navigation capabilities for low-cost marine receiver configurations.

The rapid development of new GNSS capabilities requires ongoing investigations and understanding by space weather researchers to quantify, predict and mitigate potential impacts on the integrity, accuracy and reliability of evolving user applications. Space weather hazard strategies attempt to capture such conditions of high impact (e.g. polar patches, storm enhanced density and aurora) for system users and operators. Characterization of ionospheric phenomena resulting from space weather events is key to such studies, with knowledge of ionospheric electron density distribution translating directly into effects on GNSS transionospheric signal propagation.

In this paper we highlight ionospheric disturbances for current and emerging GNSS applications, associated impacts, and consider the context of recent national efforts to advance space weather strategies and action plans. For example, in 2019 the United States conducted (as part of its national space weather action plan) a review of ionospheric disturbances benchmarks critical to vulnerability assessments for national infrastructure and services, and for stakeholder mitigation planning. The intention was to capture physical properties of the medium and to define several key parameters best characterizing the space environment: these included TEC, spatial/temporal variations of TEC, peak electron density, peak height of electron density, turbulence measures (scintillation), and signal absorption. All such values translate readily into impacts on existing and emerging systems.

We also quantify aspects of PNT accuracy and integrity using both our real data networks and our extensive GNSS simulation tools that translate key parameters into user/operator impacts. It is critically important to ensure that these tools include state-of-the-art current and future GNSS receiver designs and navigation algorithms in order to determine extreme impacts on users. Our examples include 1) ionospheric large-scale phenomena specification and structures within, both spatially and temporally, 2) small-scale irregularity specification affecting GNSS signal propagation, and 3) translating the impact of such phenomena into various user domains.

2. INTRODUCTION

With new Global Navigation Satellite System (GNSS) constellations emerging from Europe, Russia and China, there are more than 150 navigation satellites currently transmitting more than 500 L-band multi-frequency signals globally. All such signals and systems are susceptible to propagation effects in the Earth's ionosphere (Fig. 1), the part of the upper atmosphere ionized by extreme ultraviolet (EUV) and x-ray solar radiation. The resulting ionospheric electron density extends 80-1200 km altitude with three main regions: the lower D layer (60-90 km) present primarily during the day; the E layer (90-140 km) with intermittent patches of enhanced ionization; and the F region (above 140 km) with the largest electron density values typically at peak heights of 350-400 km. Ionospheric response is driven by solar emissions, and the evolution of ionospheric electron content varies in space and time: e.g. with solar cycle, season, local time and geographic location.

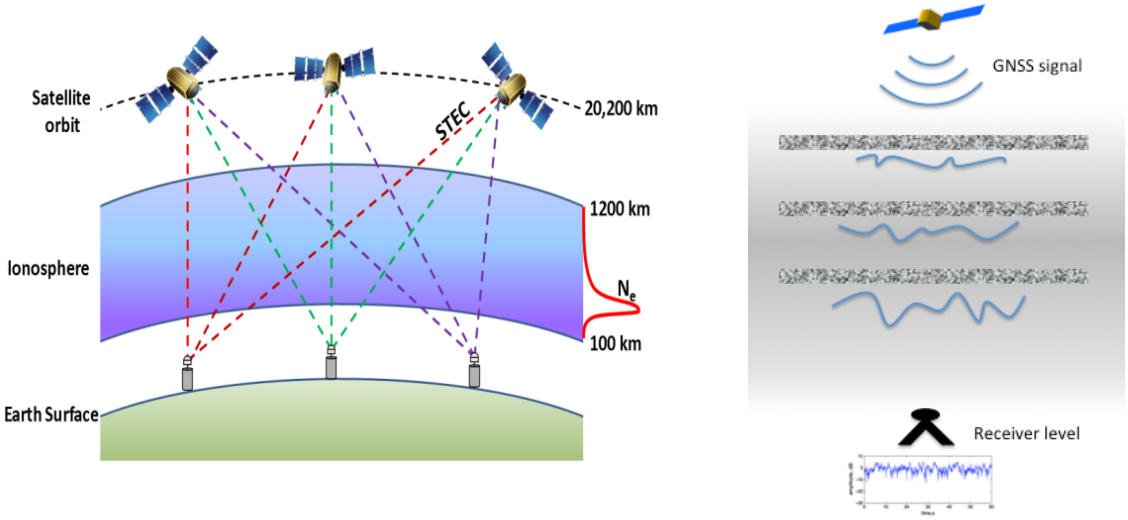

Figure 1. Large-scale transionospheric propagation of GNSS signals (left) and small-scale scintillation effects on signal phase and amplitude (right).

GNSS signals are refracted by the dispersive ionosphere as a function of signal frequency (f) and electron density along the signal path, translating into a range error expressed as

$$I = \frac{40.3}{f^2} TEC \tag{1}$$

where the slant total electron content (TEC) is defined as the integration of the electron density N_e along the signal path:

$$TEC = \int_{path} N_e ds \tag{2}$$

Ionospheric delay is thus proportional to the line integral of the free electron distribution in a 1-m^2 column along the satellite-receiver signal path, and inversely proportional to the square of the signal frequency being transmitted. Other sources of GNSS ranging error include satellite clock and orbit errors, multipath, and receiver noise. GNSS signals can also experience random rapid phase and intensity variations as they propagate through small (m-km) scale ionospheric structures in electron density [1,2] called scintillations. The effects of phase and amplitude scintillation include GNSS receiver disruptions in signal tracking and, in extreme cases, loss of navigation capabilities entirely [3].

Often the large-scale ionospheric effects are reduced through models, differential techniques, or dual-frequency ionosphere-free combinations. For decades, networks of differential GNSS (DGNSS) reference stations have operated worldwide, providing real-time range corrections that are communicated to mobile GNSS users in the local region (typically within 500 km range). The spatially correlated corrections, such as ionospheric range errors, are reduced at the user receiver for improved PNT accuracy; such systems have supported safety-critical maritime

navigation worldwide, e.g. [4], with legacy systems continuing to operate in many countries. Similarly, satellite-based augmentation systems (SBAS) generate wide area differential GNSS corrections from multiple reference stations which are uploaded to, and transmitted by, geostationary satellites across user regions spanning thousands of kilometers. For example, the Wide Area Augmentation System (WAAS) [5] and the European Geostationary Navigation Overlay Service (EGNOS) [6] are satellite-based augmentation (SBAS) approaches that provide ionospheric corrections for commercial aviation over North America and Europe.

More recently, ubiquitous multi-frequency GNSS signals have enabled stand-alone precise point positioning (PPP) approaches. The PPP solution exploits precise GNSS satellite clock and orbit corrections, with dual-frequency ionosphere-free observations, to achieve decimeter-level or better positioning accuracy with no base station required. The latest generation GNSS receivers can track 550+ signals simultaneously from five constellations, offering PNT accuracies of decimeters to meters depending on the positioning mode (Table 1).

Table 1: Typical Marine Receiver PNT Accuracies [7]

PNT Mode	Method	Horizontal Positioning Accuracy (RMS)
Standalone single point	Single frequency	1.5 m
	Dual frequency ionosphere-free	1.2 m
Differential GNSS (DGNSS)	Differential corrections (single reference station)	1 m
Satellite-based augmentation system (SBAS)	Wide area differential corrections	1 m
Precise Point Positioning (PPP)	Carrier phase multi-frequency ionosphere-free	5-10 cm

All such approaches are susceptible to increased ionospheric propagation errors during space weather events. For example large gradients in TEC can generate ten-fold increases in differential GNSS positioning errors exceeding system thresholds [8]. Scintillations in the Canadian Arctic have resulted in compromised navigation capabilities for low-cost marine single-frequency receiver configurations [9]. Studies have shown the effects of scintillation on GNSS signal propagation and system performance [10,11,12,13], particularly during moderate to strong geomagnetic storm periods. The potential threats of such storms for GNSS applications have been quantified for extreme space weather threats, including their effects on aviation, road and maritime navigation, rail transport and oil drilling [14].

We note that new frontiers in GNSS applications are advancing rapidly, to the extent that technology is out-pacing integrity. Legacy methods must be extended from traditional safety-critical navigation systems (e.g. aviation and marine) to ubiquitous autonomous platform applications and beyond [15]. Integrity has traditionally benefitted from the use of differential and/or SBAS techniques together with relevant system integrity information generated by the service provider [4]. In PPP applications the framework of a resilient PNT system can include (augmented) GNSS observations in conjunction with additional measurements available from other terrestrial-based radio-navigation systems and/or from on-board multi-sensors (e.g., inertial measurements, cameras, odometers, etc.). When augmented GNSS observations are combined with additional, non-GNSS measurements, a much more robust navigation solution can be designed in which the user is also protected from the effects of ionospheric error sources. In investigating ionospheric effects on GNSS, we take such considerations for the domain user applications into account.

3. KEY IONOSPHERIC PHENOMENA AND PARAMETERS

The rapid development of new GNSS capabilities and user needs require ongoing investigations by space weather researchers to quantify, predict and mitigate potential impacts on the integrity, accuracy and reliability of evolving user applications. Space weather events and resulting ionospheric disturbances are driven by the solar-terrestrial interaction. National space weather hazard strategies attempt to capture such conditions of high impact for system users and operators [16]. Characterization of ionospheric phenomena resulting from space weather events is key to such studies [17], with knowledge of ionospheric electron density distribution translating directly into effects on GNSS signal propagation and associated user applications. Here we highlight key phenomena and the key parameters that characterize their impact on PNT.

3.1 Storm-Enhanced Density (SED)

The ionospheric phenomenon of storm-enhanced density (SED) has been observed and studied extensively. Ionospheric gradients associated with such effects are some of the largest ever observed on Earth with gradients of 50-70 ppm in the vicinity of this effect (compared with 1-2 ppm for quiet time conditions) [18,19]. SED develops due to local electric fields in the afternoon-to-evening local time sector. Near-equatorial peaks in electron density expand to mid-latitudes where they are swept west in the latitude range 35-45 degrees geographic, towards local noon. Near local noon the electrons are driven north in the global convection pattern, northwest from the United States through Canadian latitudes, and over the pole. This is primarily an afternoon local time effect for North America. The result is a narrow plume of enhanced electrons extending from the mid- to high-latitudes, with very large TEC gradients at the edges of this feature. For a given event, this plume generally expands west from central Canada through the Pacific region over a period of several hours.

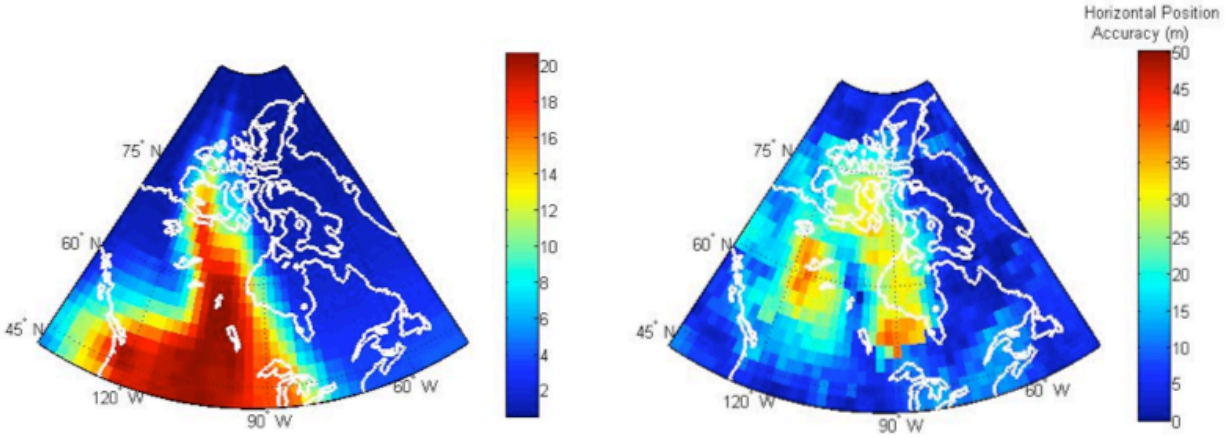

Figure 2. Ionospheric delay map for severe space weather event with storm-enhanced density (left) and SBAS GNSS horizontal positioning accuracies (right).

Fig. 2 shows the SED feature and corresponding SBAS differential GNSS positioning errors over North America. Larger PNT errors are observed in the east-west TEC gradients at the SED boundaries, with magnitudes of 30 m far exceeding typical SBAS accuracies of 1-2 m (e.g. Table 1). These results suggest that spatial TEC gradients readily translate into PNT error predictions.

3.2 High Latitude Effects

In the high latitudes, there two main regions, the polar cap and the auroral oval, in which important magnetospheric-ionospheric processes occur and initiate space weather. These regions are not fixed in space but rather have boundaries that evolve due to changing conditions in the interplanetary magnetic field (IMF) and the solar wind. Interaction of the solar IMF and terrestrial magnetic lines can result in some energetic particles entering the Earth's magnetosphere (Fig. 3). Energy deposition depends on the orientation of IMF: a parallel (south-north) orientation to the Earth's magnetic field line allows only a very small fraction of solar energetic particles to enter; an anti-parallel

(north-south orientation) generates magnetic reconnection opening the terrestrial environment to solar energetic particles. The driving magnetospheric dynamics occur across multiple scales and map primarily to the auroral oval on closed magnetic field lines and to the polar cap on open magnetic field lines. What results are variations of ionospheric parameters, such as total electron content (TEC), on multiple temporal and spatial scales [10].

The two primary issues for GNSS users are phase scintillation and sudden jumps in range measurements due to abrupt changes in TEC. Scintillation is produced by ionospheric irregularities that form in response to solar and geomagnetic events. In the high latitudes, they are primarily related to polar cap patches and the SED tongue-of-ionization (in the polar ionosphere) and particle precipitation (in both auroral and polar ionospheres). The propagation of GNSS signals through these irregularities is affected by large TEC fluctuations and (primarily) phase scintillation [20,21,22,23]. Large changes in TEC have been observed associated with aurora and have been reported by [24] and [25].

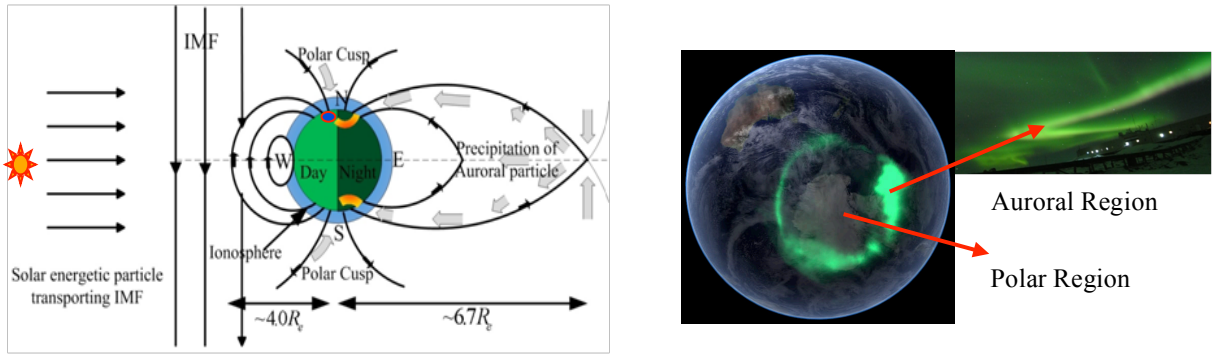

Figure 3. Solar-terrestrial interaction with Earth's atmosphere (left) and image of auroral oval (right).

Such space weather effects have been studied extensively in Arctic regions of North America with characterization of extreme space weather events [26,27,28]. Fig. 4 shows the impact on a transionospheric GNSS signal experiencing strong phase variations in an auroral arc. Auroral propagation effects on PNT are captured in measures of ionospheric turbulence or scintillation. A case study is presented in Section 5.1.

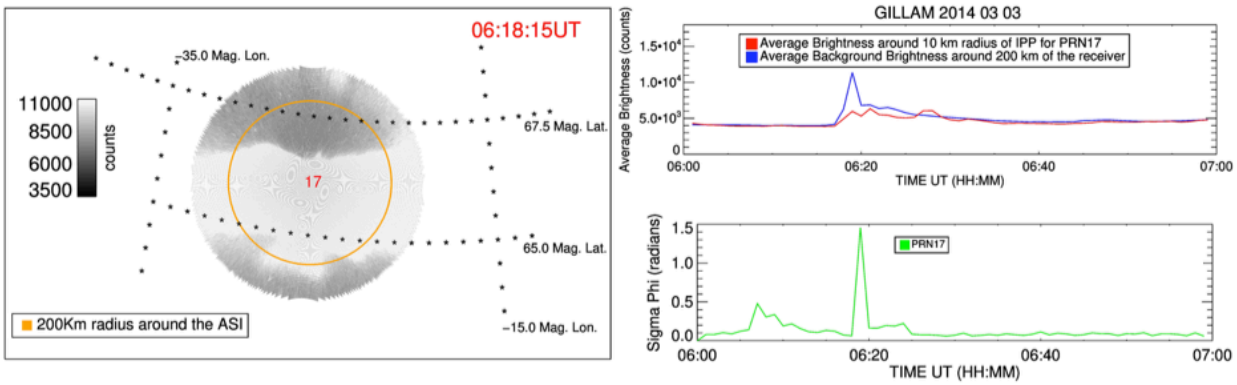

Figure 4. GPS satellite PRN 17 observations at TREx site Gillam on 3 March 2014 at 6:18 UT when the satellite ionospheric pierce point was "crossing" the auroral arc (left) and the corresponding arc brightness (upper right) and phase scintillation (lower right).

3.3 Low Latitude Regions

During evening hours, the interaction between the ionospheric eastward dynamo electric fields and the Earth's northward magnetic field results in an upward "E-cross-B" drift near the equator lifting ionospheric F-region electrons. Due to gravity, and pressure from upper layers, the elevated electrons eventually move downward - along local magnetic field lines - forming Equatorial Anomaly peaks(s) in electron density extending roughly 20 degrees either side of the magnetic equator [29]. Large TEC gradients observed at the edges of this feature [30] are associated with larger TEC gradients, scintillation and PNT positioning errors.

Equatorial scintillations are principally associated with electron density irregularities formed in the ionospheric F-region after sunset. As the F-region plasma moves to higher altitudes, vertical density gradients increase resulting in the formation of plasma density depletion areas (also known as plasma bubbles) in the lower F-region. When a bubble starts to grow or move upward, large electron density gradients on the bubble edges produce smaller irregularities. These small irregular regions with sizes on the order of the first Fresnel zone radius (~260 m for the GPS L1 signal) or less can cause strong amplitude scintillations of GNSS signals [31,32,33].

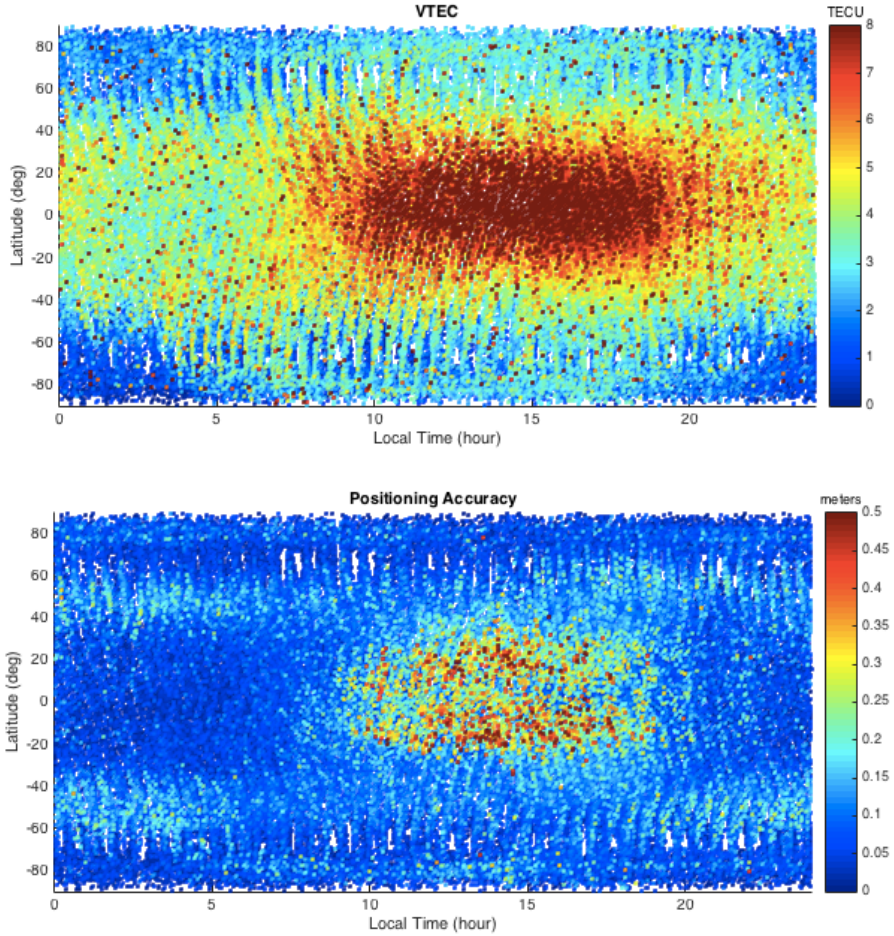

Figure 5. Over-the-satellite vertical TEC values for Swarm satellite A (upper plot) and positioning residuals (lower plot) for GPS precise point positioning approach. Values were generated at 10-minute intervals for full year of data 2018.

We provide here an example for LEO orbit determination. The European Space Agency Swarm mission, consisting of three LEO satellites (A, B and C) in polar orbits (450-550 km altitude), was launched November 2013. [34] noted consistently larger PNT residual errors for orbit determination near the geomagnetic equator associated with structured TEC and ionospheric scintillation. We processed one year of publicly available data from the precise-orbit-determination GPS receiver to 1) derive the topside (above-satellite) ionospheric TEC, and 2) investigate

precise point positioning errors at low latitudes. Fig. 5 shows the topside vertical TEC (VTEC) mapped in latitude and local time for a full year of Swarm A observations. The equatorial anomaly feature is observed in the daytime hours local time, with large spatial gradients 20 degrees N and S of the geomagnetic equator. Corresponding positioning errors of 30-40 cm exceed the typical PPP decimeter-level accuracies in Table 1.

3.4 Key Parameters

In 2018 the United States defined benchmarks for five space weather phenomena critical to vulnerability assessment for national infrastructure and services, and for stakeholder mitigation planning. The national Space Weather Strategy and Action Plan [16] subsequently included a Phase 1 "next steps space weather benchmark" review for the five identified phenomena. In the context of threat mitigation, a next-phase national working group in benchmarking of *ionospheric disturbances* provided recommendations to capture physical properties of the medium characterizing the propagation environment. Several key parameters were determined that best characterize the impact on PNT: **TEC, spatial variations of TEC, rate-of-TEC (ROTI) and turbulence measures** [35]. These naturally align with the high-impact phenomena in this section and space domain awareness aligned with service provider requirements, e.g. [36]. All such key parameters can be quantified via forecasting and now-casting methods, described by regional maps and 3D ionospheric imaging, and translate readily into impacts for existing and emerging satellite-based navigation systems.

We note that, while widely popular within the GNSS community, scintillation indices were not considered the most effective parameters for predicting or capturing physical characteristics of ionospheric irregularities and associated turbulence. Such scintillation indices are frequency and geometry dependent, typically observed for L-band, and also depend on instrument processing intervals and de-trending filters used. It was therefore recommended [35] that a system-independent ionospheric turbulence measure C_kL [37] (where C_k is the 1 km cross-section of the power-spectral density of the ionospheric irregularity and L is the thickness of the irregularity layer) be employed in future for ionospheric disturbance benchmarking and parameterization.

4. QUANTIFYING IMPACT

We employ dedicated instruments and GNSS simulation tools that account for the full range of ionospheric propagation conditions and PNT methods to observe key parameters and translate propagation effects into user/operator impacts. Our tools include testbeds and state-of-the-art current and future GNSS receiver designs and navigation algorithms in order to determine extreme impacts on various use cases. Real-world observations are combined with our GNSS hardware and software simulations to generate impact estimates for marine, aviation, land and space applications. We describe our approaches here.

4.1 Transition Region Explorer (TREx) Network

The University of Calgary's Transition Region Explorer (TREx) network is an $8M investment in over 40 new (deployed 2019-2020) sophisticated optical, magnetic and radio instruments across Canada (Fig. 6). Combined with our modeling tools, this is one of the world's foremost high latitude facilities for remote sensing of the near-earth space environment. All key parameters can be derived that characterize the ionosphere medium for radio propagation. The ground-based infrastructure includes 18 auroral cameras (6 near-infrared, 6 "blueline" and 6 true colour RGB), eleven imaging riometers (for high energy precipitation), and two spectrographs (for proton aurora). At distributed key locations within the target region, nine multi-constellation GNSS TEC/scintillation receivers and four front-end RF samplers are deployed to provide scientific observations and assess the safety-critical failure modes resulting from space weather. Commercial SBAS aviation and marine DGNSS receivers are co-located at key sites for real world testing of PNT operations.

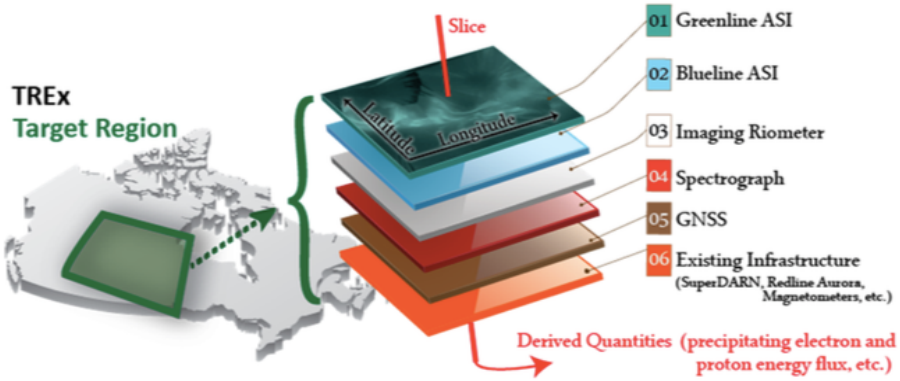

Figure 6. The University of Calgary's Transition Region Explorer (TREx) network: an $8M investment (federal and provincial funding) for remote sensing of the near-earth space environment over Canada. Ground-based infrastructure includes co-located multi-spectral All-Sky Imagers (ASI), ground-based GNSS receivers, and riometers for simultaneous measurement of ionospheric precipitation, absorption, and plasma variations.

By exploiting available multi-instrument multi-scale observations from this dense network, multi-structured phenomena may be resolved and the space environment characterized with the resolution necessary to parameterize high-impact threats. In-the-field testing of commercial systems and their internal integrity monitoring allows identification of real-world anomalous behaviour. For example, the largest magnitude ionospheric propagation errors may be readily rejected as outliers by internal receiver integrity monitoring (with minimal user impact for precise PNT) while smaller signal perturbations may skew navigation solutions (as they accumulate over time) beyond acceptable error bounds for some marine PNT receivers. Our observing capabilities, combined with our TECMODELG3 software package for ionospheric TEC estimation, provide unique opportunity to study a wide range of physical drivers, ionospheric response, and impact on PNT performance.

4.2 Simulation Tools

Estimated or observed parameter values for space weather phenomena are translated into system impacts via our modeling approaches, hardware simulators and software receivers – such that space weather threats can be investigated for a variety of use cases. For example, Fig. 7 shows ionospheric perturbations (real data or simulated) superposed on nominal GNSS digital signal samples. Our GNSS software receiver, GSNRx, is capable of processing GNSS multi-frequency multi-constellation signals in all PNT modes. The receiver acquires and tracks the incoming raw GNSS signals and generates a number of measurements, including the carrier and code phase, which can then be processed in various navigation algorithms – simulating all receiver architectures from low-cost marine systems to multi-frequency precise point positioning (sub-decimeter level accuracy) systems. This approach allows us to derive risk indicators for any given PNT system and to develop representative use cases for land, marine, aviation and/or space applications.

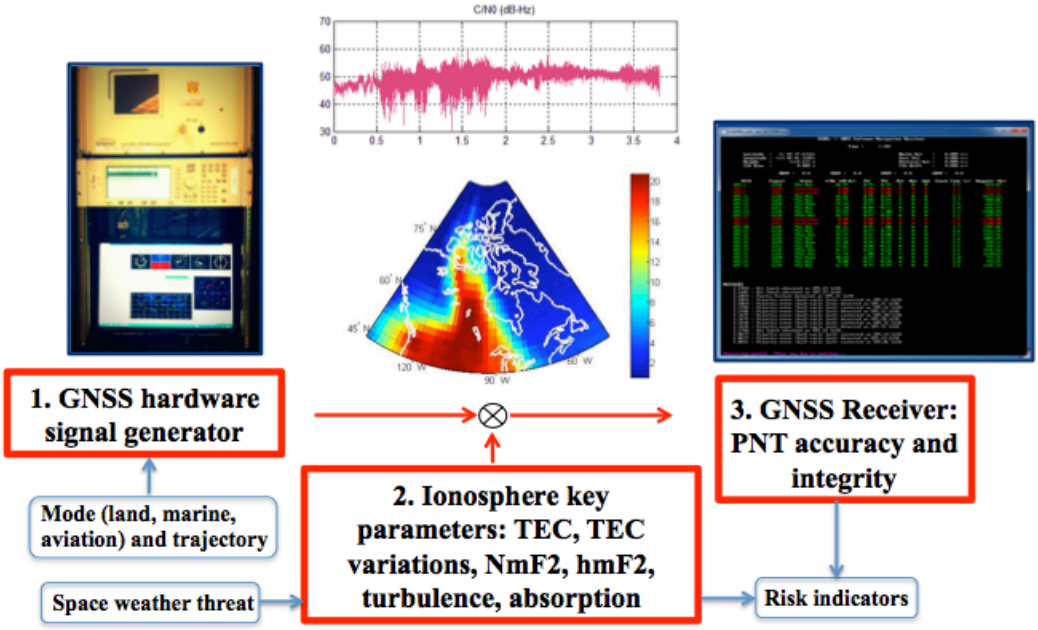

Figure 7. Integrated hardware and software approaches to estimate space weather impact for various PNT modes (land, marine, aviation) via 1) generating nominal GNSS signals, 2) superposing ionospheric effects defined by key parameters for a given space weather threat, and 3) software receiver signal processing in stand-alone, differential GNSS, SBAS or precise point positioning approaches to generate PNT errors and error bounds.

Our physics-based phase screen model accepts scintillation or C_kL input values describing properties of the ionospheric irregularities with additional flexibility for computing transionospheric propagation parameters based on frequency, geometry, dynamics, etc. This model allows wider implementation to assess space weather impact on a range of GNSS architectures and applications, and even UHF to C band propagation analysis. Such advanced simulation tools are also necessary to comprehensively investigate the full range of space weather impacts including multi-frequency correlations [38] for the modernized and new GNSS constellations.

5. CASE STUDIES

We translate space weather threats into RF signal propagation and impact for representative case studies using our testbed TREx datasets and augmentations. We consider real-world operator and user needs including not only PNT accuracy but also system/service availability and integrity. For example, Tables 2 and 3 show examples of several PNT requirements stated in the U.S. Federal Radio Navigation Plan [36] for national infrastructure and user applications. With respect to emerging technologies, the FRP notes many systems and services requiring precise in-vehicle positioning and navigational support. The next-generation transportation systems, such as connected vehicles and automated vehicles, will rely even more on GNSS. The FRP suggests PNT solutions consisting of GNSS combined with other subsystems in the vehicle to deliver accuracies in range of 10 cm horizontal (95%). We note that national infrastructure requirements also include precision timing reliant on GNSS. The tables provided show thresholds established for safety of navigation (accuracy) and service disruption (availability) for a few FRP user domains. We consider ionospheric disturbances and associated impacts in this context.

Table 2. Sample User Positioning and Navigation Requirements [36]

Requirements	Horizontal Accuracy (95%, 2DRMS)	Availability	Time to Alert	Integrity (Alert Limit)
Maritime restricted waterways	2-5 m	99.9%	N/A	N/A
Highway navigation and route guidance	1-20 m	>95%	5 s	2-20 m
Connected vehicle initiative	10 cm	99.9%	5 s	0.2 m

Table 3. Sample Timing Requirements [36]

Requirements	Accuracy (95%)
Telecommunications timing	340 ns

5.1 Maritime Systems

As shown in Tables 2 and 3, maritime radio navigation systems must comply with safety-critical standards often expressed in terms of accuracy and availability. All such specifications are defined statistically. For example, Table 2 defines requirements of 2-5 m horizontal positioning accuracy 2DRMS (95%) with 99.9% availability for ships navigating restricted waterways. Marine differential GNSS receivers may be challenged to meet such requirements during space weather events. An example is given here (Fig. 8) where auroral particle precipitation causes ionospheric variability with increased GNSS differential range errors and some scintillated GNSS signals. PNT vulnerability is assessed in terms of the 2DRMS (95%) accuracy thresholds. Larger positioning errors are due to ionospheric disturbances and anomalies in the receiver autonomous integrity monitoring – where receiver algorithms are amplifying rather than mitigating ionospheric errors; the duration of this event is five minutes (less than 0.1% daily) which does not compromise system availability.

Having identified this receiver anomalous behaviour we characterized the nature of the ionospheric disturbance through generating rate-of-TEC (ROTI) values at a GNSS site within our TREx network (see [21] and [39] for full ROTI description). This ROTI parameter was measured for six months to assess GNSS marine user vulnerability. ROTI is assumed to characterize the ionospheric properties correlated with the larger GNSS signal perturbations [37] and the PNT errors in Fig. 8 as established in previous studies [27]. The propagation environment is then simulated in terms of observed ROTI parameters and the differential GNSS positioning impact assessed for the marine receiver processing. This enables translation of measured physical ionospheric characteristics of TEC variations directly into user system impact and assessment of risk indicators (Fig. 9).

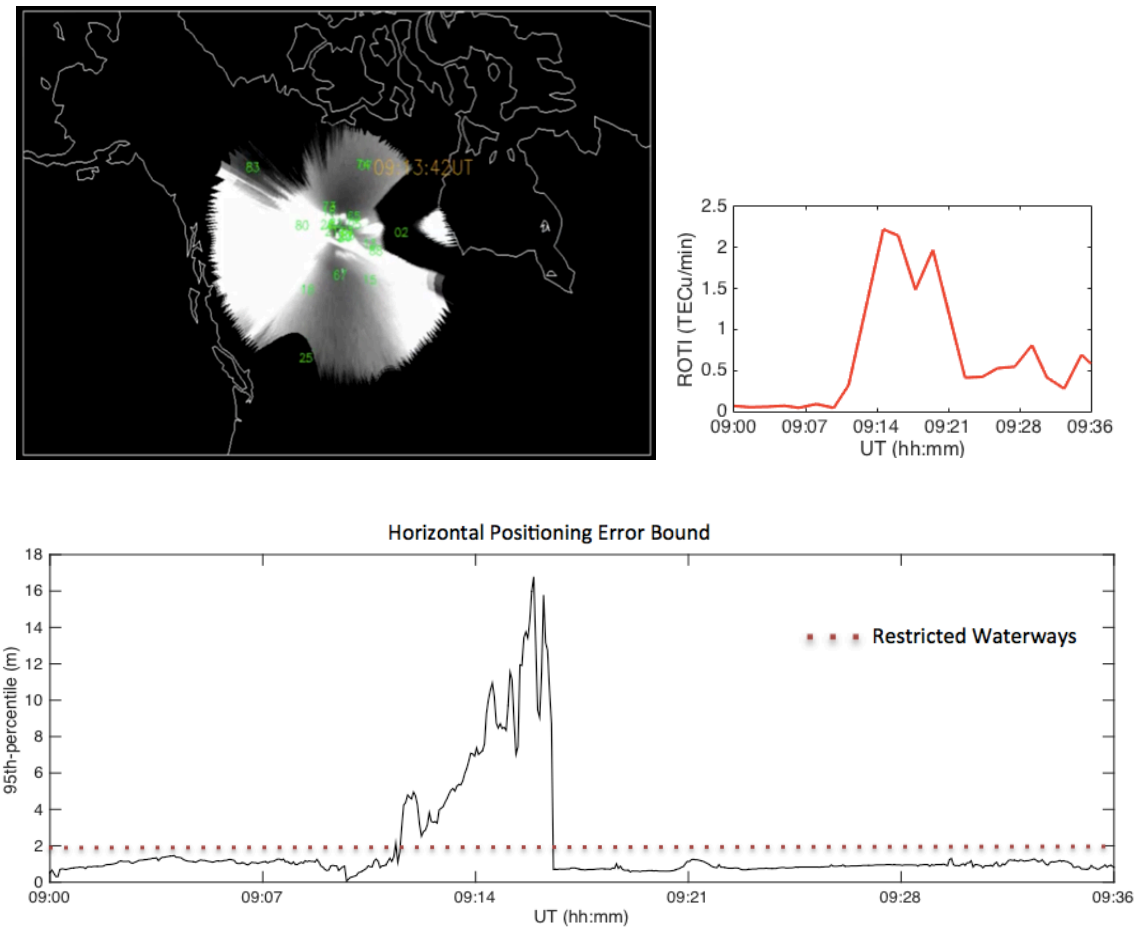

Figure 8. GPS satellite signals propagating through aurora (green pierce points in all-sky image, upper plot) and corresponding rate-of-TEC increases (upper plot, right) and increases in horizontal positioning error (lower plot) for a maritime GNSS system. Larger positioning errors are due to ionospheric disturbances and anomalies in the receiver processing – where receiver algorithms are likely amplifying rather than mitigating ionospheric errors. Normal receiver function provides navigation accuracy better than 2 m (2DRMS, 95%).

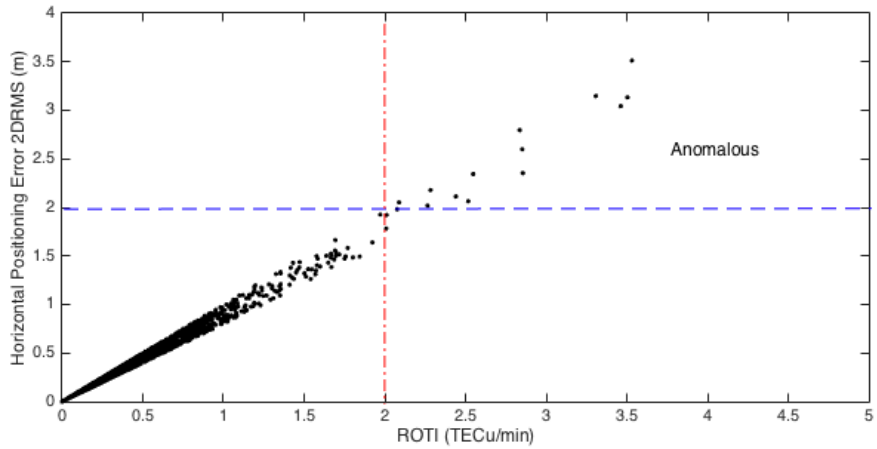

Figure 9. Marine horizontal positioning accuracy as a function of ionospheric TEC variability (ROTI). Position errors greater than 2 m (95% probability) exceed normal system behavior and are attributed to space weather threats.

When observed ROTI values exceed a risk threshold of 2 TECu/min (Fig. 9), marine horizontal positioning errors are predicted to exceed 2 m (95% probability). A ROTI risk indicator can therefore identify probability of anomalous behaviour for such safety-critical PNT systems. Monitoring space weather and/or ionosphere parameters in this manner, and establishing risk indicator thresholds, allows operators to estimate potential system impact and even differentiate between the presence of natural versus human-made threats. Maps of ROTI in this manner (forecast or now-cast) could provide specific user information regarding the level of navigation accuracy and availability and/or general warnings.

We further investigated multi-constellation solutions to mitigate such PNT errors. A persistent ionospheric TEC structure with ROTI exceeding 2 TECu/min was simulated and the resulting ionospheric propagation effects superposed on nominal GNSS signals. Simulated signals were then processed by the GNSS receiver, with investigation of internal algorithms for three controlled scenarios: GPS only, GPS+GLONASS, and GPS+GLONASS+Galileo. Results are shown in Fig. 10. For GPS only, the receiver is unable to identify and reject the scintillation-induced error and continues to process a corrupt observation. For GPS+GLONASS the anomalous error is reduced through the additional satellite observations. When the Galileo signals are included, observation redundancy is sufficient for the receiver internal integrity monitoring to reject the outlier and achieve sub-meter positioning accuracy (well within the marine navigation requirements in Table 2).

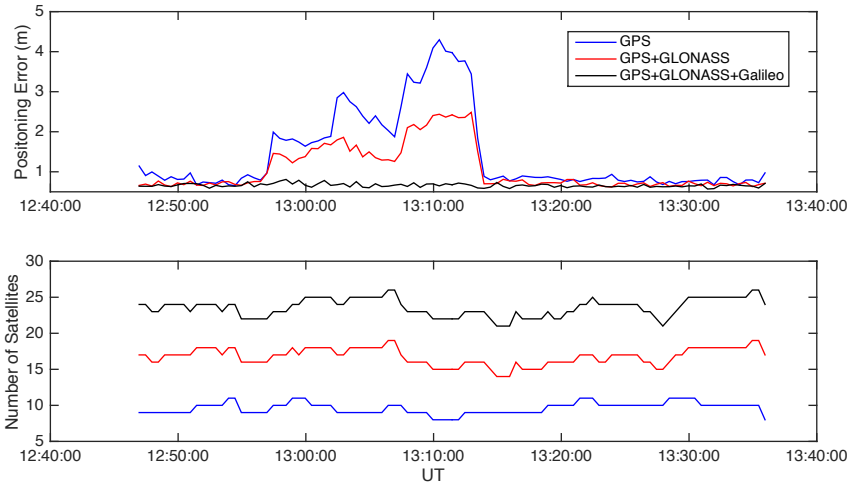

Figure 10. Marine receiver horizontal positioning errors for GPS-only and multiple constellation methods (upper plot) and corresponding number of GNSS satellites used in positioning solution (lower plot).

5.2 Precise Point Positioning

As an example of scintillation impact on emerging applications, Fig. 11 shows auroral image data from a UCalgary all-sky imager [40,41] in northern Canada. Spatial resolution of this 256 pixel wide image is ~1 km at zenith assuming the aurora at an E-region altitude of 110 km. The complementary GPS data were obtained from a nearby commercial GPS scintillation receiver. Phase scintillation indices provide information about plasma variations in the ionosphere propagation medium; the index σ_ϕ is standard deviation of detrended GNSS signal phase observations. When such measurements are combined with auroral images, a greater understanding of the causal physical phenomena can be gained.

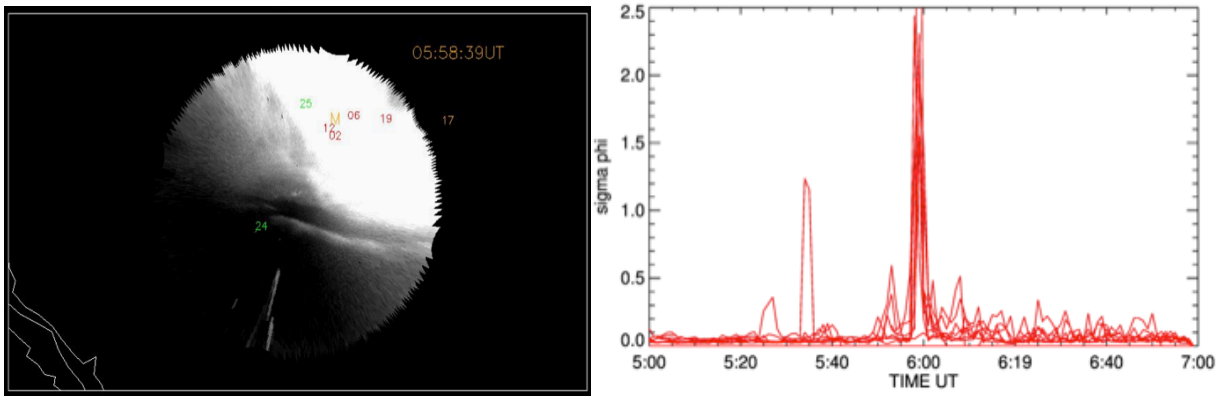

Figure 11. Auroral image (left) at 5:55 UT, 2 March 2017, from all-sky imager at Athabasca. GPS PRN numbers (in green and red) show locations of signal ionospheric pierce points inside an auroral arc, and corresponding phase scintillation indices (right) for all satellites in view 5:00-7:00 UT.

In this real world case study, surface mining operations for natural resource extraction were disrupted due to discontinuities in GPS precise positioning services during the auroral activity. Fig. 12 shows the percentage of ambiguity resets for local GPS carrier phase observations. The GPS observations are degraded for signals propagating through the edges of quickly evolving auroral arcs. The GPS carrier phase residuals during the period of auroral activity are at decimeter-level compared with centimeter-level during periods of minimal ionospheric activity.

We investigate such PNT errors through extended TREx scintillation/turbulence observations and simulation of precise positioning algorithms. Fig. 13 shows ten months of GNSS phase scintillation observations for TREx site Fort Smith (60 deg N latitude, 111.9 deg W longitude). Most values are below 0.2 rad, reflecting the absence of ionospheric disturbances, with the larger values of 1-2 rad measured when aurora, such as that in Fig. 11, are present. Approximately a dozen auroral events were detected in the data set. In simulation these observed scintillation estimates were used to drive turbulence models [42] generating signal perturbations then superposed on nominal GPS signals for a simulated static user. A standard precise point positioning approach was implemented to estimate PNT errors. High scintillation values resulted in tenfold increases in navigation errors consistent with our real-world test case. A further simulation included augmenting GNSS with inertial sensors for redundancy and bridging of GNSS observation gaps. For the simple static user case simulated here, the addition of inertial relative motion information resulted in reductions of positioning errors – primarily by enabling outlier detection and rejection and bridging GNSS gaps. In the context of future autonomous systems we suggest further rigorous studies to assess integrity performance.

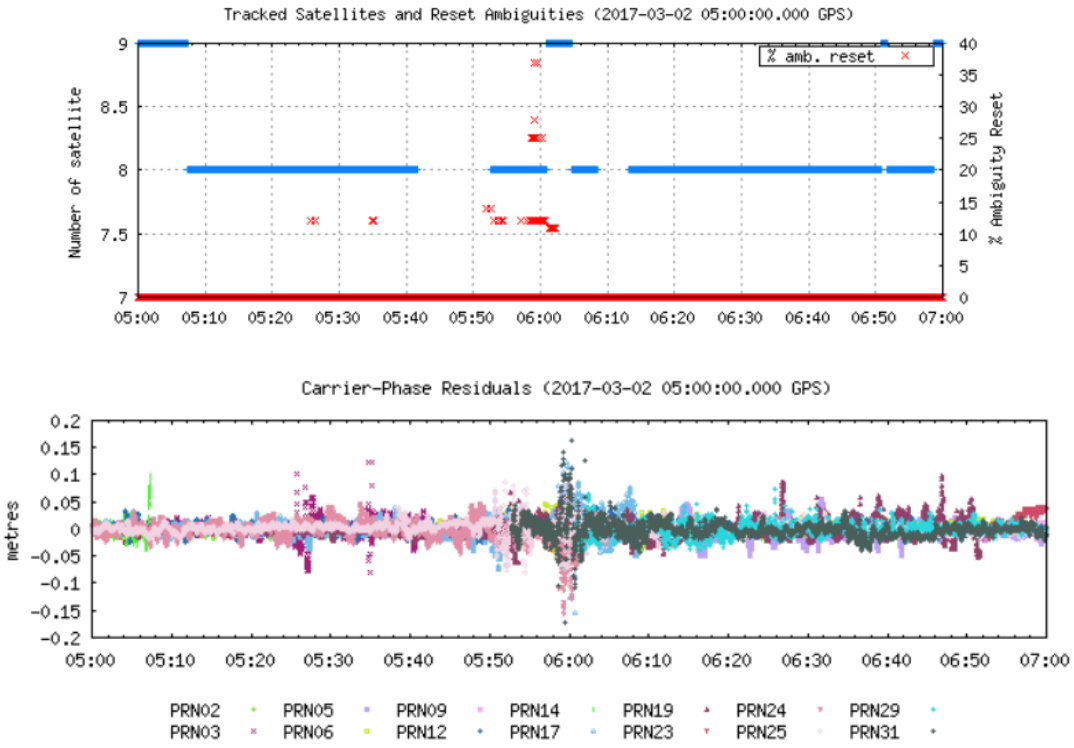

Figure 12. Number of satellites (blue) and percentage of carrier phase ambiguity resets (red) on 2 March 2017 (upper plot) and GPS carrier phase residuals (lower plot).

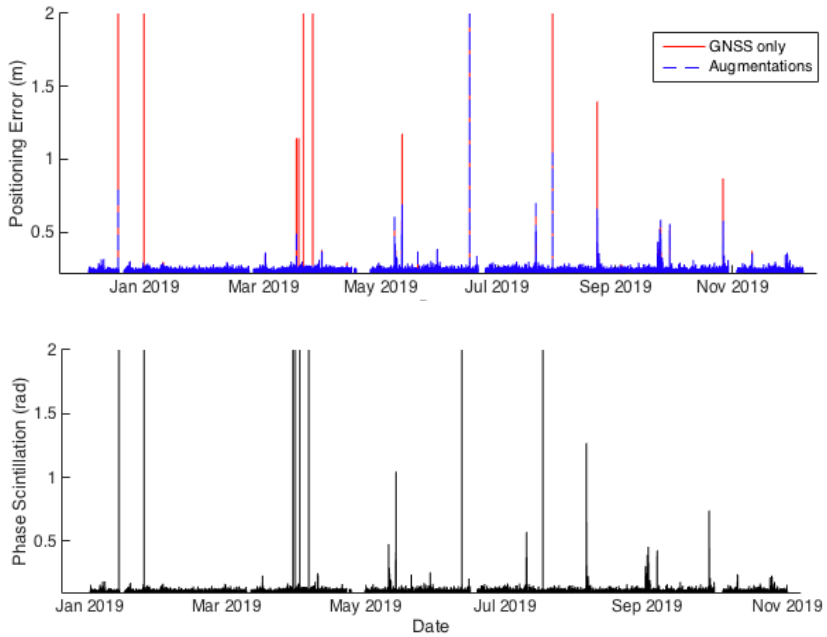

Figure 13. Precise point positioning solutions using GPS+GLONASS (upper plot, red) and GPS+GLONASS+INS (upper plot, blue) simulations, driven by GPS phase scintillation observations (lower plot) at TREx site Fort Smith.

6. SUMMARY

Society relies increasingly on capabilities that are enabled or delivered by space-based systems, and there exists a need to continually refine our vulnerability assessment models and our understanding of natural threats. One area of focus is monitoring and mitigating hazards for space-based systems that are highly dependent on the space atmospheric environment - which includes the magnetosphere, thermosphere, and the ionosphere. The United States has developed national space weather strategies to address existing and emerging threats to satellite-based infrastructure, signals and services, among others. Preparing for space weather events is critical for technology innovations that rely on transionospheric signals and GNSS is notable in this respect – with widespread applications in positioning, navigation and timing.

GNSS signals are refracted and diffracted by ionospheric electron density along the signal path, with ranging errors dependent on the total electron content. These effects are generally mitigated through models, differential techniques, or dual-frequency ionosphere-free combinations. All such methods are less effective, however, when ionospheric phenomena generate structured electron content variations. At the larger end of the spatial scale are the equatorial anomaly, storm-enhanced density, and highly energetic geomagnetic storms and sub-storms that couple energy into the polar regions resulting in aurora and sub-auroral ionospheric disturbances. At the small end of the spatial scale are less energetic phenomena, such as traveling ionospheric disturbances, sporadic-E, and auroral-E, scintillation. In this paper we describe various phenomena and investigate associated PNT impacts.

The very large TEC gradients at storm-enhanced density boundaries can generate differential positioning errors exceeding 30 m, well beyond the thresholds of accuracy requirements for safety-critical transportation systems. It is noted that such events are rare and do not compromise overall PNT service availability. Signal perturbations due to scintillations can degrade PNT accuracy at high and low latitudes; magnitudes of positioning errors are typically meter-level for such space weather phenomena. We note in particular the vulnerability of applications relying on precise point positioning approaches. This method depends primarily on precise carrier phase observations which are susceptible to signal disruptions and loss of signal lock – requiring reset and divergence of the navigation filter generating meters of positioning error. Some receiver architectures may exhibit anomalous behavior, with internal integrity algorithms unable to detect and reject the corrupt observations, with errors exceeding thresholds of system accuracy requirements.

With rapidly emerging new frontiers of PNT, there is a focus on integrity and an ongoing trend of translating the well-consolidated integrity concept from aviation to other market domains, e.g. for autonomous and connected vehicles. This will require a tight integration of GNSS with all onboard sensors, integrating not only absolute positioning but also relative motion information. In the context of such multi-sensor technologies, close coordination of the scientific communities with operators and service providers is beneficial for identifying and mitigating space weather threats.

7. REFERENCES

[1] Yeh, K. C. and C.-H. Liu, Radio wave scintillations in the ionosphere, *Proceedings of the IEEE*, vol. 70, no. 4, pp. 324-360, April 1982. doi: 10.1109/PROC.1982.12313.

[2] Kintner, P. M., B. M. Ledvina, and E. R. de Paula (2007), GPS and ionospheric scintillations, *Space Weather*, 5, S09003, doi:10.1029/2006SW000260.

[3] Ghafoori, F., and S. Skone, High Latitude Scintillation Analysis for Marine and Aviation Applications, *Proceedings of the 25th International Technical Meeting of The Satellite Division of the Institute of Navigation (ION GNSS 2012)*, ION, Nashville, 2013 September, pp. 2722-2730.

[4] Porretta, M., D. Jimenez Banos, M. Crisci, G. Solari, and A. Fiumara, GNSS Evolutions for Maritime: An Incremental Approach, *Inside GNSS*, pp 54-62, May/June 2016.

[5] Walter, T. K. Shallberg, E. Altshuler, W. Wanner, W. J. Hughes, C. Harris and R. Stimmler, WAAS at 15, *Proceedings of the 31th International Technical Meeting of The Satellite Division of the Institute of Navigation (ION GNSS 2011)*, September 2018.

[6] ESSP-DRD-25591P: European Satellite Services Provider (ESSP) EGNOS Service Provision Yearly Report (April 2019–March 2020) ESSP; Toulouse, France: July 2, 2020.

[7] Veripos: New Marine Receiver Delivers Ultra-precise Position, *Inside GNSS*, May 2020.

[8] Skone, S. and A. Coster, Studies of storm-enhanced density impact on DGPS using IGS reference station data, *Journal of Geodesy*: Volume 83, Issue3, Page 235, 2008, doi:10.1007/s00190-008-0242-9.

[9] Coster, A., S. Skone, D. Hampton and E. Donovan, Monitoring Space Weather with GNSS Networks Expanding GNSS Networks into Northern Alaska and Northwestern Canada, *Proceedings of the 30th International Technical Meeting of The Satellite Division of the Institute of Navigation (ION GNSS+ 2017)*, Portland, Oregon, September 2017.

[10] Forte, B., C. Coleman, S. Skone, I. Häggström, C. Mitchell, F. Da Dalt, T. Panicciari, J. Kinrade, and G. Bust, Identification of scintillation signatures on GPS signals originating from plasma structures detected with EISCAT incoherent scatter radar along the same line of sight, J. Geophys. Res.Space Physics, 122, 916–931, 2017, doi:10.1002/2016JA023271.

[11] Strangeways, H. J., Y. Ho, M. H. O. Aquino, Z. G. Elmas, H. A. Marques, J. F. G. Monico and H. A Silva, On determining spectral parameters tracking jitter and GPS position improvement by scintillation mitigation, *Radio Science*, *46*, 2011, doi:10.1029/2010RS004575.

[12] Tiwari, R., H. J. Strangeways, S. Tiwari and A. Ahemad, Investigation of ionospheric irregularities and scintillation using TEC at high latitude, *Advances in Space Research,* 52(6), pp. 1111-1124, 2013.

[13] Jacobsen, K. S. and S. Schafer, Observed effects of a geomagnetic storm on an RTK positioning network at high latitudes, *J. Space Weather Space Clim*, 2, A13, 2012, doi.org/10.1051/swsc/2012013

[14] Cannon, P., Royal Academy of Engineering, Extreme space weather: impacts on engineered systems and infrastructure, Annual Report, January, 2013.

[15] Vani, B., B. Forte, J. Monico, S. Skone, M. Shimabukuro, A. Moraes, I. Portella and H. Marques, A novel approach to improve GNSS Precise Point Positioning during strong ionospheric scintillation: theory and demonstration, *IEEE Transactions on Vehicular Technology*, March 2019, doi: 10.1109/TVT.2019.2903988.

[16] National Science and Technology Council, National Space Weather Strategy and Action Plan, March 2019, at https://www.whitehouse.gov/wp-content/uploads/2019/03/National-Space-WeatherStrategy-and-Action-Plan-2019.pdf

[17] Coster, A., S. Skone, D. Hampton, E. Donovan and A. Weatherwax, New Cyberinfrastructure for GNSS Ionospheric Scintillation and Total Electron Content Parameters,"*Proceedings of the 31st International Technical Meeting of The Satellite Division of the Institute of Navigation (ION GNSS+ 2018)*, Miami, Florida, September 2018, pp. 4102-4110, doi.org/10.33012/2018.15920.

[18] Coster, A. and S. Skone, "Monitoring Storm-Enhanced Density using IGS Reference Station Data", Journal of Geodesy, Volume 83, Number 3-4, pp 345-351, 2009, doi.org/10.1007/s00190-008-0272-3.

[19] Haddad, O., Skone, S., Sparks, L., WAAS Performance Investigation for Disturbed Ionospheric Conditions over Canadian Latitudes, *Proceedings of the 24th International Technical Meeting of The Satellite Division of the Institute of Navigation (ION GNSS 2011)*, Portland, OR, September 2011, pp. 2462-.

[20] Basu. S, S. Basu, and E. Mackenzie (1985), Morphology of Phase and Intensity Scintillations in Auroral Oval and Polar Cap, *Radio Science*, 20(3), 347-356, doi: 10.1029/RS020i003p00347.

[21] Pi. X, A. J. Mannucci, U. J. Lindqwister, and C. M. Ho, Monitoring of global ionospheric irregularities using the worldwide GPS network, *Geophysical Research Letters*, 24(18), pp. 2283–2286, 1997, doi: 10.1029/97GL02273.

[22] Kintner, P. M., B. M. Ledvina, and E. R. de Paula, GPS and ionospheric scintillations, *Space Weather*, 5(S09003), 2007, doi: 10.1029/2006SW000260

[23] Ghafoori, F. and S. Skone, High latitude scintillation analysis for marine and aviation applications", Proceedings of the 25th *International Technical Meeting of The Satellite Division of the Institute of Navigation (ION GNSS 2012)*, Nashville, TN, Sep 2012, pp. 2722-2730.

[24] Semeter, J., S. Mrak, M.Hirsch, J. Swoboda, H. Akbari, G. Starr, D. Hampton, P. Erickson, F. Lind, A. Coster, and V. Pankratius, GPS signal corruption by the discrete Aurora: Precise measurements from the Mahali experiment. Geophysical Research Letters, 44, 9539–9546, 2017, doi.org/10.1002/2017GL073570.

[25] Mrak, S., J. Semeter, M. Hirsch, G. Starr, D. Hampton, R. H. Varney, A. S. Reimer, J. Swoboda, P. J. Erickson, F. Lind, A. J. Coster and V. Pankratius, Field-aligned GPS scintillation: Multisensor data fusion. Journal of Geophysical Research: Space Physics, 123, 974–992, 2018, doi.org/10.1002/2017JA024557.

[26] Mushini, S. C., S. Skone, E. Spanswick, E. Donovan, and M Najmafshar, Proxy index derived from All Sky Imagers for space weather impact on GPS, *Space Weather*, 16, pp. 838–848, 2018, doi:10.1029/2018SW001919.

[27] Pi, X., A.J. Mannucci, B. Valant-Spaight, Y. Bar-Sever, L.J. Romans, S. Skone, L. Sparks, L. Hall and G. Martin, Observations of Global and Regional Ionospheric Irregularities and Scintillation Using GNSS Tracking Networks, *Proceedings of the ION 2013 Pacific PNT Meeting*, ION, Honolulu, Hawaii, 2013 April, pp 752-761.

[28] Linty, N., Minetto, A., Dovis, F. and L. Spogli, Effects of phase scintillation on the GNSS positioning error during the September 2017 storm at Svalbard. Space Weather, 16, 1317–1329, 2018, doi.org/10.1029/2018SW001940

[29] Kendall, P. and D. Windle, The Appleton Anomaly. *Nature* **207,** 964–965, 1965, https://doi.org/10.1038/207964a0

[30] Pradipta, R. and P. Doherty, Assessing the Occurrence Pattern of Large Ionospheric TEC Gradients over the Brazilian Airspace, *NAVIGATION*, Vol 63, Issue 3, pp 335-343, Fall 2016, doi.org/10.1002/navi.141.

[31] Basu, B., Characteristics of electromagnetic Rayleigh‐Taylor modes in the nighttime equatorial plasma, J. Geophys. Res., 110, A02303, 2005, doi:10.1029/2004JA010659.

[32] Zernov N.N., V.E. Gherm and H.J. Strangeways, On the effects of scintillation of low latitude bubbles on transionospheric paths of propagation, *Radio Science*, 44:RS0A14, 2009, doi:10.1029/2008RS004074.

[33] Muella, M., E. A. Kherani, E. R. de Paula, A. P. Cerruti, P. M. Kintner, I. J. Kantor, C. N. Mitchell, I. S. Batista and M. A. Abdu, Scintillation‐producing Fresnel‐scale irregularities associated with the regions of steepest TEC gradients adjacent to the equatorial ionization anomaly, *J Geophys Res: Space Physics*, Vol. 115, Issue A3, March 2010.

[34] van den IJssel *et al. Earth, Planets and Space,* 68:85, 2016, doi: 10.1186/s40623-016-0459-4.

[35] IDA Group Report NS GR-10982, *Next Step Space Weather Benchmarks*, commissioned report in fulfillment of the United States National Space Weather Strategy and Action Plan, December 2019, Chair: G. Reeves, Theme Leaders: C. Cohen, D. Gary, D. Jackson, P. Riley, and S. Skone.

[36] U.S. Federal Radionavigation Plan 2019: DOT-VNTSC-OST-R-15-01.

[37] Carrano, C. S., K.M. Groves and C.L. Rino, On the relationship between the rate of change of total electron content index (ROTI), irregularity strength (CkL), and the scintillation index (S4). *Journal of Geophysical Research: Space Physics*, 124, 2099–2112, doi.org/10.1029/ 2018JA026353, 2019.

[38] Sokolova, N., A. Morrison and J. Curran, Do modern multi-frequency civil receivers eliminate the ionospheric effect?, *GNSS Solutions*, pp. 34-39, 2017.

[39] Cherniak, I., A. Krankowski and I. Zakharenkova, ROTI Maps: a new IGS ionospheric product characterizing the ionospheric irregularities occurrence, GPS Solutions, 22(3), July 2018, doi: 10.1007/s10291-018-0730-1.

[40] Donovan. E., S. Mende, B. Jackel, H. Frey, M. Syrjasuo, I. Voronkov, T. Trondsen, L. Peticolas, V. Angelopoulos, S. Harris, M. Greffen and M. Connors, The THEMIS All-Sky Imager Array - System design and initial results from the prototype imager, *J. Atmos. Solar Terr. Phys*., 68, pp. 1472–1487, 2006, doi:10.1016/j.jastp.2005.03.27.

[41] Mende. S, S. E. Harris, H. U. Frey, V. Angelopoulos, C. T. Russel, E. Donovan, B. Jackel, M. Greffen and L. M. Peticolas, The THEMIS array of ground-based observatories for the study of auroral substorms, *Space Science Reviews*, 141(1-4), pp. 357-387, 2008, doi:10.1007/s11214-008-9380-x.

[42] Ghafoori, F. and S. Skone, Impact of equatorial ionospheric irregularities on GNSS receivers using real and synthetic scintillation signals, Radio Science, Vol. 50, Issue 4, pp 294-317, April 2015, doi.org/10.1002/2014RS005513.